American Mineralogist, Volume 97, pages 1314–1319, 2012

Redetermination of high-temperature heat capacity of Mg_2SiO_4 ringwoodite: Measurement and lattice vibrational model calculation

Hiroshi Kojitani,[1,*] Madoka Oohata,[1] Toru Inoue,[2] and Masaki Akaogi[1]

[1]Department of Chemistry, Faculty of Science, Gakushuin University, 1-5-1 Mejiro, Toshima-ku, Tokyo 171-8588, Japan
[2]Geodynamics Research Center, Ehime University, 2-5 Bunkyo-cho, Matsuyama 790-8577, Japan

Abstract

Isobaric heat capacities (C_P) of Mg_2SiO_4 forsterite and ringwoodite were measured by differential scanning calorimetry in the temperature range of 306–833 K. The measured C_P of Mg_2SiO_4 forsterite was consistent with those reported by previous studies. On the other hand, the present C_P of Mg_2SiO_4 ringwoodite was about 3–5% larger than those measured by previous researchers. The calorimetric data of Mg_2SiO_4 ringwoodite were extrapolated to 2500 K using a lattice vibrational model calculation, which well reproduced the low-temperature C_P data measured by thermal relaxation method. The calculated C_P shows good agreement with the present calorimetric data. The obtained C_P was expressed by the polynomial of temperature: $C_P = 164.30 + 1.0216 \times 10^{-2}T + 7.6665 \times 10^{3}T^{-1} - 1.1595 \times 10^{7}T^{-2} + 1.3807 \times 10^{9}T^{-3}$ [J/(mol·K)] in the range of 250–2500 K.

Keywords: Mg_2SiO_4, ringwoodite, heat capacity, DSC, Kieffer model calculation, thermodynamic property, mantle transition zone

Introduction

It is widely accepted that magnesium-rich $(Mg,Fe)_2SiO_4$ olivine, which is the most abundant mineral in the Earth's upper mantle, transforms to wadsleyite and then ringwoodite in the mantle transition zone and, furthermore, ringwoodite dissociates into magnesium-rich $(Mg,Fe)SiO_3$ perovskite and ferropericlase at the 660-km boundary between the transition zone and the lower mantle. Therefore, thermodynamic property of Mg_2SiO_4 ringwoodite, which is the dominant end-member of the ringwoodite phase, is key to understand the Earth's structure from the mantle transition zone to the uppermost lower mantle.

In a thermodynamic calculation, isobaric heat capacity (C_P) is necessary to calculate enthalpy and entropy at high temperatures from those at standard state (298.15 K). Because C_P data of Mg_2SiO_4 ringwoodite observed at high temperatures have been limited to only those reported by Watanabe (1982) and Ashida et al. (1987) using the differential scanning calorimetry (DSC), many researchers have used the C_P based on them for thermodynamic calculations (e.g., Akaogi et al. 1984; Fei and Saxena 1986; Bina and Wood 1987; Saxena et al. 1993; Jacobs and Oonk 2001; Fabrichnaya et al. 2004). However, results of a lattice dynamics calculation by Price et al. (1987), of a lattice vibrational model calculation based on Raman spectroscopy by Chopelas et al. (1994) and of ab initio calculations by Yu and Wentzcovitch (2006) and Ottonello et al. (2009) indicated larger C_P than those obtained in the two experimental studies beyond the experimental errors. Recently, Akaogi et al. (2007) measured low-temperature C_P of Mg_2SiO_4 ringwoodite in a temperature range of 2–305 K with thermal relaxation method using the Physical Property Measurement System (PPMS). The C_P by Akaogi et al. (2007) showed about 4% larger value than that of Ashida et al. (1987) in a range of 210–300 K. These discrepancies have required a re-determination of high-temperature C_P of Mg_2SiO_4 ringwoodite.

There are two methods to obtain C_P from DSC data, namely, "scanning method" and "enthalpy method" (Mraw and Naas 1979). In the scanning method, C_P of a sample is determined using a ratio of heat flow signal intensity from a baseline for the sample to that for a standard (e.g., α-Al_2O_3) at a certain temperature during a temperature scan. The two previous measurements (Watanabe 1982; Ashida et al. 1987) adopted this method. On the other hand, in the enthalpy method, C_P is determined by dividing heat content by temperature difference during a scan. The heat content is obtained by integrating an area surrounded by a heat flow signal and a baseline over the scan duration. Mraw and Naas (1979) recommended the enthalpy method because of established equilibrium initial and final temperatures before and after energy input, respectively, which eliminate uncertainties from sample temperature lag during the scan. In this study, C_P of Mg_2SiO_4 forsterite and Mg_2SiO_4 ringwoodite were measured by the differential scanning calorimetry in a temperature range of 306–833 K using the enthalpy method. Obtained C_P data of Mg_2SiO_4 ringwoodite were extrapolated to temperatures higher than 830 K using the lattice vibrational model calculation.

Experimental methods

Sample preparation

Single crystal of Mg_2SiO_4 forsterite for a starting material of high-pressure synthesis of Mg_2SiO_4 ringwoodite was synthesized using the Czochralski method. It was crushed and ground into powder. High-pressure synthesis of Mg_2SiO_4 ringwoodite was made using a Kawai-type multi-anvil high-pressure apparatus at GRC, Ehime University. A Pt heater-capsule was used. For details of the high-pressure high-temperature technique, see Higo et al. (2006). The starting sample

* E-mail: hiroshi.kojitani@gakushuin.ac.jp

0003-004X/12/0809–1314$05.00/DOI: http://dx.doi.org/10.2138/am.2012.4054

of Mg_2SiO_4 forsterite was held at 22 GPa and 1473 K for 1 h and then temperature quenched and decompressed to ambient pressure. The recovered sample was crushed and ground into powder. Mg_2SiO_4 forsterite used for C_P measurement was synthesized by heating a mixture of reagent-grade MgO and SiO_2 powder with a mole ratio of 2:1 at 1773 K for 130 h in air. Powder X-ray diffraction measurements of the synthesized samples confirmed that they were single phases of Mg_2SiO_4 ringwoodite and Mg_2SiO_4 forsterite, respectively. The lattice parameter of the synthesized Mg_2SiO_4 ringwoodite was determined to be a = 8.0647(2) Å, which is the same within the uncertainties as 8.0649(1) Å reported by Sasaki et al. (1982). The composition analysis of the Mg_2SiO_4 ringwoodite sample using a scanning electron microscope with an energy-dispersive spectrometer (SEM-EDS) showed that there was no impurity and that its composition was stoichiometric.

Heat-capacity measurement

Heat capacity of Mg_2SiO_4 ringwoodite was measured using a differential scanning calorimeter (DSC) (PerkinElmer Diamond DSC). Calorimetric temperature was calibrated using the melting points of indium, tin, and zinc. A purge gas of nitrogen was flown during the measurements. In the temperature range from 298 to 573 K, the heating rate was 10 K/min and data were obtained with a step of 5 K. In the range 553–843 K, the step was 20 K with a heating rate of 20 K/min. Data acquisition interval was 1 s. α-Al_2O_3, which was prepared by heating a reagent-grade chemical at 1773 K for 12 h in air, was used as the calorimetric standard. The weights of Mg_2SiO_4 forsterite, Mg_2SiO_4 ringwoodite, and α-Al_2O_3 samples were 12.68, 10.56, and 14.04 mg, respectively. Each sample was packed in an aluminum pan. In a calorimetric run, a set of measurements for the empty pan, α-Al_2O_3 and Mg_2SiO_4 forsterite/Mg_2SiO_4 ringwoodite was made in a temperature range of about 100 K . Observed heat data were analyzed using the enthalpy method (Mraw and Naas 1979). At each step, the middle temperature was taken as the measurement one. Heat capacities for Mg_2SiO_4 forsterite and ringwoodite were calibrated by those for α-Al_2O_3 obtained just before each measurement using heat capacity data of α-Al_2O_3 by Ditmars et al. (1982). Three to seven data measured at each temperature were averaged.

Results and Discussion

Heat capacity of Mg_2SiO_4 forsterite and ringwoodite

The results of C_P measurements of Mg_2SiO_4 forsterite are shown in Table 1 and Figure 1. The C_P values are compared with well-constrained previous data determined using the adiabatic calorimetry of Robie et al. (1982), the DSC measurements of Watanabe (1982) and Ashida et al. (1987), and the least-squares fitting to heat content data of Orr (1953) where the Maier-Kelley equation, $C_P = a + bT + cT^{-2}$, was used for the fitting. The C_P values measured in this study agree with those by the previous workers within the discrepancies of about 0.6%, except for only the data by Ashida et al. (1987). Their data indicate smaller values than the others, particularly in the range of 450–620 K with average discrepancy of 1.2%. Our data are very close to those by Orr (1953) and also show good agreement with C_P proposed by Gillet et al. (1991), which was based on their high-temperature heat content measurements above 780 K. These facts strongly suggest that the C_P data measured in this study are reliable.

Table 1. Isobaric heat capacities of Mg_2SiO_4 forsterite measured using differential scanning calorimetry

T (K)	C_P [J/(mol·K)]	T (K)	C_P [J/(mol·K)]	T (K)	C_P [J/(mol·K)]
306	118.6(6)	421	140.7(11)	536	153.0(6)
311	119.7(9)	426	141.1(11)	541	153.3(4)
316	121.1(10)	431	141.7(11)	546	153.7(5)
321	122.2(12)	436	142.1(12)	551	154.1(4)
326	123.4(12)	441	143.2(11)	556	154.5(4)
331	124.5(11)	446	144.1(11)	561	154.8(6)
336	125.7(11)	451	145.1(13)	566	155.3(4)
341	126.5(13)	456	146.5(19)	571	155.7(4)
346	128.1(12)	461	146.3(9)	576	156.1(4)
351	129.0(11)	466	145.9(11)	581	156.5(7)
356	129.9(12)	471	146.6(10)	586	156.8(6)
361	130.8(12)	476	147.5(7)	591	157.4(7)
366	131.7(12)	481	147.9(12)	633	158.7(17)
371	132.8(11)	486	148.4(14)	653	159.9(15)
376	133.6(12)	491	148.9(12)	673	161.1(17)
381	134.3(12)	496	149.5(5)	693	162.3(16)
386	135.0(12)	501	150.1(5)	713	163.2(18)
391	135.9(12)	506	150.7(7)	733	163.9(19)
396	136.7(12)	511	150.7(9)	753	165.0(19)
401	137.4(11)	516	151.1(6)	773	165.5(21)
406	138.8(18)	521	151.6(5)	793	166.4(20)
411	139.3(11)	526	152.1(5)	813	167.0(24)
416	140.1(10)	531	152.5(6)		

Note: Errors in parentheses are twice the standard deviation of the mean.

C_P values of Mg_2SiO_4 ringwoodite measured in this study are listed in Table 2. Experimental errors were ±0.5–2.6%, depending on temperature. In Figure 2, they are compared with those measured by Watanabe (1982) and Ashida et al. (1987) using DSC. Our C_P data are 3–5% larger than those observed by Ashida et al. (1987) over the temperature range of 300–700 K. As mentioned above, the C_P data for Mg_2SiO_4 forsterite above 400 K by Ashida et al. (1987) are about 0.5–2% smaller than those constrained by the present and the other previous studies. As pointed out by previous workers (Hofmeister and Ito 1992; Chopelas 1999; Karki and Wentzcovitch 2002; Akaogi et al. 2008), C_P for $MgSiO_3$ akimotoite reported by Ashida et al. (1988), which was measured using the same calorimeter as that in Ashida et al. (1987), also contains systematic error. For example, the C_P values of $MgSiO_3$ akimotoite measured by Ashida et al. (1988) are about 4% smaller than those measured by the PPMS (Akaogi et al. 2008). Therefore, it is implied that the C_P values for Mg_2SiO_4 ringwoodite of Ashida et al. (1987) contain a similar degree of systematic error as well. Furthermore, a sintered Mg_2SiO_4 ringwoodite sample was used in the measurement of Ashida et al. (1987). Since a sintered sample has less contact with an aluminum pan than a powder of the same sample with

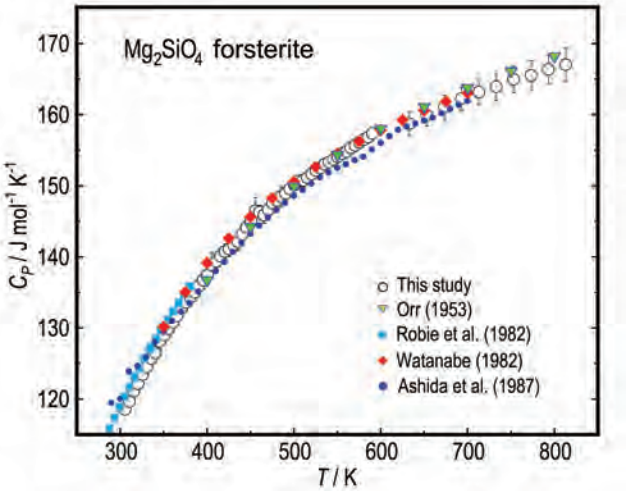

Figure 1. Comparison of heat capacity of Mg_2SiO_4 forsterite measured in this study using the differential scanning calorimetry (DSC) with those by previous calorimetric studies. Open circles show the present DSC data. Solid diamonds and solid circles are the previous DSC data reported by Watanabe (1982) and Ashida et al. (1987), respectively. Solid squares are data from adiabatic calorimetry of Robie et al. (1982). Solid inverted triangles represent re-fitted data from the least-squares fitting of the equation $C_P(T) = a + bT + cT^{-2}$ to heat content data by Orr (1953). (Color online.)

TABLE 2. Isobaric heat capacities of Mg_2SiO_4 ringwoodite measured using differential scanning calorimetry

T (K)	C_P [J/(mol·K)]	T (K)	C_P [J/(mol·K)]	T (K)	C_P [J/(mol·K)]
306	117.2(12)	436	141.0(6)	556	153.0(14)
311	118.4(12)	441	141.5(6)	561	153.7(14)
316	119.9(11)	446	142.0(6)	563	153.5(12)
321	121.3(12)	451	142.4(7)	566	153.9(12)
326	122.6(12)	456	142.5(10)	571	154.6(9)
331	123.8(11)	461	144.1(6)	583	154.9(10)
336	124.9(11)	466	144.7(7)	603	156.5(10)
341	126.0(11)	471	145.3(5)	623	157.9(13)
346	127.2(11)	476	145.5(6)	643	158.8(13)
351	128.5(15)	481	146.0(7)	653	159.5(30)
356	129.3(13)	486	146.6(7)	663	160.0(13)
371	130.3(13)	491	146.8(11)	673	160.9(27)
376	131.1(14)	496	147.3(14)	683	161.3(13)
381	132.2(12)	501	147.7(10)	693	161.7(29)
386	133.1(12)	506	148.2(13)	703	162.0(13)
391	135.1(7)	511	148.5(10)	713	162.8(30)
396	135.9(9)	516	149.2(13)	733	163.8(31)
401	136.7(7)	521	149.5(11)	753	164.5(32)
406	136.9(7)	526	150.1(13)	773	165.4(32)
411	137.8(9)	531	150.6(12)	793	166.5(34)
416	138.1(8)	536	151.1(14)	813	167.1(33)
421	139.0(5)	541	151.3(12)	833	167.9(35)
426	139.7(6)	546	152.1(14)		
431	140.4(6)	551	152.8(12)		

Note: Errors in parentheses are twice the standard deviation of the mean.

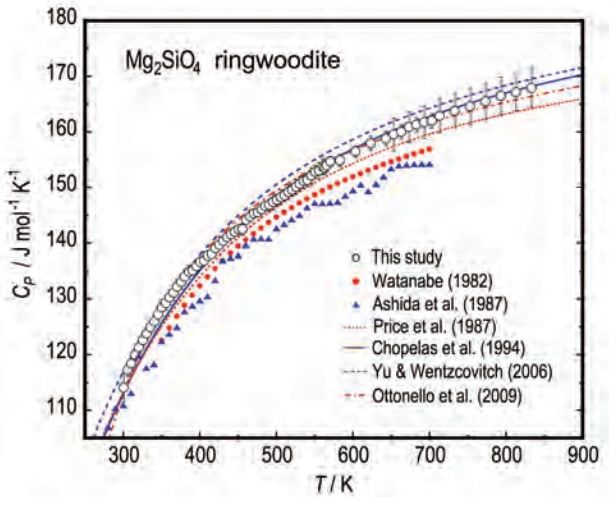

FIGURE 2. Comparison of the heat capacity of Mg_2SiO_4 ringwoodite measured in this study (open circles) with those determined by previous researchers. Solid circles and solid triangles indicate DSC data measured by Watanabe (1982) and Ashida et al. (1987), respectively. The data points of Watanabe (1982) were obtained from the fitted equation given in the literature. Dashed and dashed-and-dotted curves represent heat capacities from ab initio calculations by Yu and Wentzcovitch (2006) and Ottonello et al. (2009), respectively. Solid and dotted curves indicate heat capacities calculated from lattice vibrational calculation by Chopelas et al. (1994) and lattice dynamics calculation by Price et al. (1987), respectively. (Color online.)

the same weight, the sample temperature lag from the monitored temperature for the former is probably larger than that for the latter. This means that, in the scanning method for analysis of observed heat data, C_P of the sintered sample would not be correctly calibrated by that observed with powdered α-Al_2O_3 standard because of the difference in the sample temperature lag between them. Hence, their use of the sintered Mg_2SiO_4 ringwoodite sample would be another possible explanation for the large deviation from our data.

The C_P values for Mg_2SiO_4 ringwoodite reported by Watanabe (1982) are 2–4% smaller than the present results, as well as those by Ashida et al. (1987). Although the reasons of the difference between Watanabe's (1982) data and ours are not clear, the following issue may be suggested. The Mg_2SiO_4 ringwoodite sample used in Watanabe (1982) was synthesized in a Ni-Cr capsule. If a little amount of Ni component was contained in the Mg_2SiO_4 ringwoodite sample, it might partly contribute to his smaller C_P values because the use of the formula weight of pure Mg_2SiO_4 for a $(Mg,Ni)_2SiO_4$ solid-solution sample provides a larger mole number of the sample, resulting in a smaller molar heat capacity.

The present C_P data show good agreement with those determined especially from the vibrational model calculation by Chopelas et al. (1994) and from the ab initio calculation by Ottonello et al. (2009), rather than those determined by the previous DSC measurements.

Vibrational model calculation of heat capacity

Since Mg_2SiO_4 ringwoodite is stable at pressures higher than about 18 GPa at 1700 K, heating above 900 K at ambient pressure results in back transformation to Mg_2SiO_4 forsterite (Akaogi et al. 1984). For this reason, measured C_P data of Mg_2SiO_4 ringwoodite above 830 K were not available. Therefore, the high-temperature C_P data determined in this study were extrapolated to 2500 K by a vibrational model calculation using the Kieffer model (Kieffer 1979a, 1979b) taking into account the low-temperature C_P measured by Akaogi et al. (2007).

Physical properties and parameters used in the Kieffer model calculation are listed in Table 3. Chopelas et al. (1994) modeled a vibrational density of states (VDoS) of Mg_2SiO_4 ringwoodite using several optic continua. In this study, the VDoS was represented by two optic continua considering Raman and infrared (IR) spectroscopic data by Chopelas et al. (1994), Akaogi et al. (1984), and McMillan and Akaogi (1987) and phonon dispersions from a first-principle calculation by Yu and Wentzcovitch (2006). In the Kieffer model calculation, calculated C_P in the low-temperature range below about 300 K is largely affected

TABLE 3. Vibrational density of states model and physical properties for heat capacity calculation using the Kieffer model

	Lower limit (cm^{-1})	Upper limit (cm^{-1})	Fraction
TA1	0	146*	0.0238
TA2	0	155*	0.0238
LA	0	255*	0.0238
OC1	240	600	0.7381
OC2	790	840	0.1905
Formula weight (g/mol)	140.69		
V_0 (Å^3)	131.14†‡		
Z	2†		
K_{0T} (GPa)	182(3)§		
$(\partial K_{0T}/\partial T)_P$ (GPa/K)	–0.025(1)‖		
γ_{th}	1.10#		

Note: TA: transverse acoustic mode; LA: longitudinal acoustic mode; OC: optic continuum.
* Calculated from sound velocities reported by Jackson et al. (2000) and Li (2003).
† Reduced cell.
‡ Sasaki et al. (1982).
§ Meng et al. (1994).
‖ Katsura et al. (2010).
Chopelas et al. (1994).

by the lower-cutoff frequency of the first optic continuum. The lowest frequency of optic continua for the VDoS model by Chopelas et al. (1994) is about 300 cm^{-1}, probably based on only the observed Raman and IR spectra. However, the phonon dispersions of Yu and Wentzcovitch (2006) show that the lowest frequency in the optic modes is about 230 cm^{-1} for a T_{2u} mode, which is inactive for both Raman and IR. Taking the T_{2u} mode into account, the lowest frequency of 240 cm^{-1} was chosen in this study to reproduce the low-temperature C_P data measured by Akaogi et al. (2007). As no Raman and IR band was observed between 600 and 790 cm^{-1}, the frequency region was regarded as a stopping band that is supported by the phonon dispersions of Yu and Wentzcovitch (2006). The upper cutoff of 840 cm^{-1} for the second optic continuum was determined from the Raman band of T_{2g} mode observed at 834–836 cm^{-1} (McMillan and Akaogi 1987; Chopelas et al. 1994). The first and the second optic continuum contain 31 and 8 modes, respectively (Chopelas et al. 1994). The fractions for the optic continua were calculated using them. The cutoff frequencies for the three acoustic modes were derived from the acoustic velocity data of Jackson et al. (2000) and Li (2003). C_P is calculated by adding anharmonic effect to isochoric heat capacity (C_V) obtained from the lattice vibrational model calculation, using the following equation

$$C_P = C_V + \alpha^2 K_{0T} V_T T \quad (1)$$

where α, K_{0T}, and V_T are thermal expansivity, isothermal bulk modulus, and volume at 1 atm and T K, respectively. The α for Mg_2SiO_4 ringwoodite has not yet been constrained well. For example, α equations of Suzuki et al. (1979) and of Katsura et al. (2010) give 2.53×10^{-5} and 2.72×10^{-5} K^{-1} at 600 K, respectively, and the constant α value in a temperature range of 293–973 K determined by Inoue et al. (2004) is $3.07(6) \times 10^{-5}$ K^{-1}. This causes large uncertainty in calculated C_P at high temperature. In this study, using the following thermodynamic relation

$$\alpha = \frac{\gamma_{th} C_V}{K_{0T} V_T}. \quad (2)$$

Equation 1 was changed to the expression without α

$$C_P = C_V + \frac{(\gamma_{th} C_V)^2 T}{K_{0T} V_T} \quad (3)$$

where γ_{th} represents thermal Grüneisen parameter. For the γ_{th}, a weighted average mode Grüneisen parameter, $\langle\gamma\rangle$, of 1.10 determined from high-pressure Raman spectroscopy of Chopelas et al. (1994) was used. The γ_{th} was regarded approximately as a constant value due to almost no dependency on temperature above about 500 K for mantle constituent minerals (Anderson and Isaak 1995). V_T was assumed to be constant with V_{298} because a small change in V hardly affects the resultant C_P. K_{0T} at T K was calculated using K_{0T} at 298 K ($K_{0,298}$) and its temperature derivative at constant pressure $(\partial K_{0T}/\partial T)_P$ with the following equation

$$K_{0T} = K_{0,298} + \left(\frac{\partial K_{0T}}{\partial T}\right)_P \cdot (T - 298). \quad (4)$$

The $K_{0,298}$ is tightly constrained to be ~182 GPa by high-pressure X-ray diffraction measurement of Meng et al. (1994) and calculation from K_{0S} obtained from the Brillouin scattering experiment of Weidner et al. (1984). In this study, the $K_{0,298}$ of 182(3) GPa determined by Meng et al. (1994) was adopted. $(\partial K_{0T}/\partial T)_P$ values have been reported to be –0.027(5) GPa/K by Meng et al. (1994) and –0.025(1) GPa/K by Katsura et al. (2010). The latter was used in the present calculation because it was determined based on data measured in a temperature range of 300–2000 K, which is much wider than those in the former (300–700 K).

The calculated C_P data were expressed using a polynomial of temperature proposed by Fei and Saxena (1987)

$$C_P = k_0 + k_1 T + k_2 T^{-1} + k_3 T^{-2} + k_4 T^{-3} \quad (5)$$

in a valid temperature range of 250–2500 K. Determined heat capacity coefficients are tabulated in Table 4. The calculated C_P is compared with the calorimetric data measured in this study and by Akaogi et al. (2007) in Figure 3. Errors of the C_P were estimated to be 0.4–1.7%, increasing with increasing temperature, from uncertainties of the lower-cutoff frequency of the first optic continuum (±5 cm^{-1}), γ_{th} (±0.1), K_T (±3 GPa), $(\partial K_T/\partial T)_P$ (±0.001 GPa/K), and V_{298} (±0.003 cm^3/mol). Our VDoS model reproduces well not only the low-temperature C_P data of Akaogi et al. (2007) but also the present calorimetric data. This result suggests that the C_P calculation using Equation 3 together with C_V calculated from the lattice vibrational model by taking into account low-temperature calorimetric data provides a good extrapolation to high temperature. The C_P values calculated in this study are listed in Table 5 compared with those determined from the lattice vibrational model calculation by Chopelas et al. (1994), from the ab initio calculations by Ottonello et al. (2009) and Yu and Wentzcovitch (2006), from the lattice dynamics calculation by Price et al. (1987), and the calorimetric data of this study and Akaogi et al. (2007). Although our C_P calculated above 600 K is almost the same as that calculated by Chopelas et al. (1994), the latter indicates smaller values than the former below 300 K because of their higher lower-cutoff frequency of the first optic continuum. The C_P values computed by Ottonello et al. (2009) also agree with our calculation results over the whole temperature range within the uncertainties. The results of lattice dynamics calculation by Price et al. (1987) and the ab initio calculation by Yu and Wentzcovitch (2006) indicate smaller and larger values than ours, respectively. The weighted average thermal Debye temperature, θ_{th}, of Mg_2SiO_4 ringwoodite was obtained to be 935 K for our C_V from 350 to 700 K by following the method used in Watanabe (1982). The value is smaller than 1012 K of Watanabe (1982) because of our larger C_P.

Entropy

C_P calculated with the procedure mentioned above is used to determine vibrational entropy from the following equation

TABLE 4. Heat capacity coefficients of Mg_2SiO_4 ringwoodite

$C_P = k_0 + k_1 T + k_2 T^{-1} + k_3 T^{-2} + k_4 T^{-3}$ [J/(mol·K)]				
k_0	$k_1 \times 10^2$	$k_2 \times 10^{-3}$	$k_3 \times 10^{-7}$	$k_4 \times 10^{-9}$
164.30	1.0216	7.6665	–1.1595	1.3807

Note: Valid temperature range is from 250 to 2500 K.

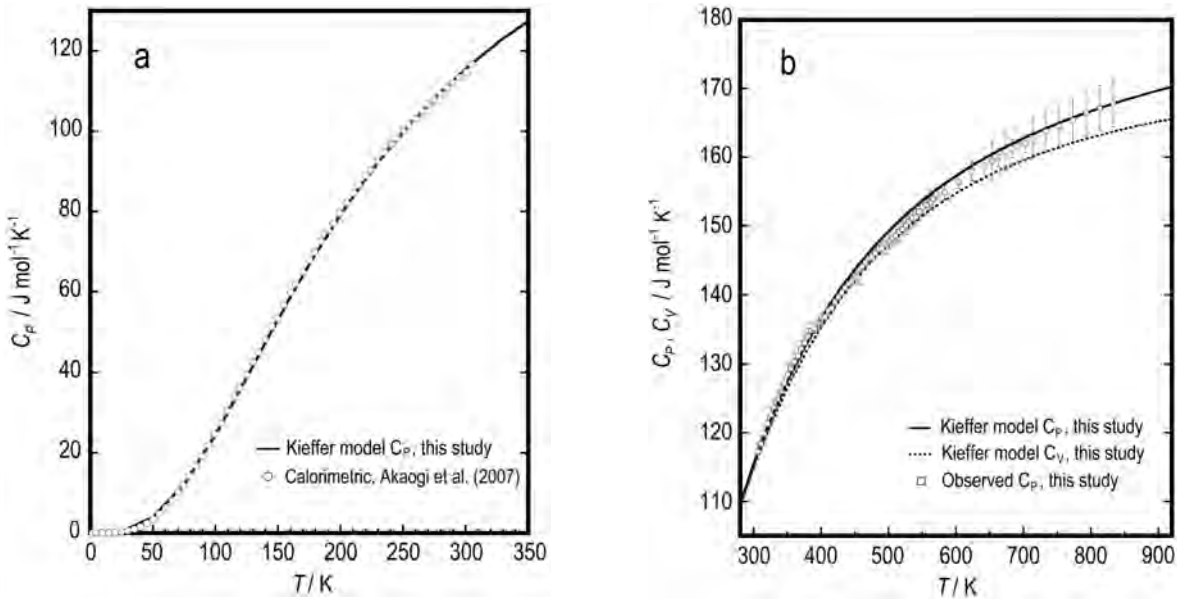

FIGURE 3. Isobaric (C_P) and isochoric (C_V) heat capacities of Mg_2SiO_4 ringwoodite calculated in this study using the Kieffer model. (**a**) In a low-temperature region of 0–350 K, the calculated C_P is compared with calorimetric data by Akaogi et al. (2007). (**b**) In a temperature region of 300–900 K, the calculated C_P (solid curve) is compared with those measured in this study. The calculated C_V is shown with a dotted curve.

TABLE 5. Results of isobaric heat capacity calculation of Mg_2SiO_4 ringwoodite, compared with those calculated by Chopelas et al. (1994), Ottonello et al. (2009), Yu and Wentzcovitch (2006), and Price et al. (1987) and those by calorimetric measurements

T	C_P^{calc} [J/(mol·K)]					T	C_P^{exp}
(K)	LVM*	LVM†	Ab initio‡	Ab initio§	LD‖	(K)	[J/(mol·K)]
50	3.99	3.66		3.84	3.37	50	3.43(3)#
100	24.45	20.39		25.54	23.76	101	25.25(7)#
150	53.22	48.10		54.99	52.19	149	53.61(13)#
200	79.18	74.95		80.98	77.62	200	79.51(15)#
300	115.5	113.0	112.9	117.0	113.2	301	114.65(30)#
400	136.6	135.2	137.3	137.9	134.0	401	136.7(7)*
500	149.2	148.5	149.4	150.5	146.5	501	147.7(10)*
600	157.3	156.9	156.7	158.6	154.3	603	156.5(10)*
700	162.8	162.7	161.6	164.2	159.6	703	162.0(13)*
800	166.7	167.0	165.3	168.4	163.2	813	167.1(33)*
900	169.7	170.3	168.3	171.5	165.9		
1000	172.1	173.0	170.8	174.1	167.9		
1200	175.8		174.9	178.3			
1400	178.7		178.2	181.8			
1600	181.2		181.1	185.0			
1800	183.5		183.5	188.1			
2000	185.7		185.6	191.4			
2500	191.5		189.5	200.8			

Note: LVM = lattice vibrational model calculation; LD = lattice dynamics calculation.
* This study.
† Chopelas et al. (1994).
‡ Ottonello et al. (2009).
§ Yu and Wentzcovitch (2006).
‖ Price et al. (1987).
Akaogi et al. (2007).

$$S_T^\circ = \int_0^T \frac{C_P}{T} dT \,. \quad (6)$$

Vibrational entropies at 298 K (S°_{298}) obtained by the present and previous studies are compared in Table 6. In this study, S°_{298} was calculated to be 82.6(7) J/(mol·K). The error was estimated by taking uncertainty of the lower cutoff frequency of the first optic continuum of ±5 cm^{-1} into account. Our value shows good agreement with that obtained from the observed data by Akaogi et al. (2007), indicating that, again, the present VDoS model well reproduces the low-temperature C_P of Akaogi et al. (2007). Also, it is comparable to that by Ottonello et al. (2009). S°_{298} determined by Chopelas et al. (1994) shows a much smaller value than the others, due to the relatively smaller C_P than measured ones below about 400 K (Table 5). In Table 7, the vibrational entropies at 1 atm and high temperatures using the C_P calculated in this study

TABLE 6. Comparison of vibrational entropy at 298 K for Mg_2SiO_4 ringwoodite among calorimetric data, vibrational model calculations, and ab initio calculation

	S°_{298} [J/(mol·K)]
This study	82.6(7)*
Akaogi et al. (2007)	82.7(5)†
Chopelas et al. (1994)	77.4(6)*
Ottonello et al. (2009)	80.2–81.7‡

* Lattice vibrational model calculation.
† Calorimetry with thermal relaxation method.
‡ Ab initio calculation.

TABLE 7. Comparison of calculated vibrational entropies of Mg_2SiO_4 ringwoodite at 1 atm and high temperatures

T (K)	S°_T (This study) [J/(mol·K)]	S°_T (Jacobs and Oonk 2001)* [J/(mol·K)]
300	83.47	83.48
400	119.82	118.39
500	151.80	148.77
600	179.80	175.37
800	226.49	220.04
1000	264.29	256.60
1200	295.99	287.53
1400	323.30	314.34
1600	347.33	338.02
1800	368.81	359.24
2000	388.28	378.48

* Values were calculated using their C_P equation based on the thermal expansivity of forsterite by Kajiyoshi (1986).

are compared with those obtained from a C_P equation of Jacobs and Oonk (2001), which was based on the calorimetric data by Watanabe (1982) and Ashida et al. (1987) and was optimized using the thermal expansivity by Kajiyoshi (1986). In the entropy calculations, S°_{298} of 82.7(5) J/(mol·K) by Akaogi et al. (2007) was used as the standard value. The entropies calculated from our C_P are about 3% larger above 600 K than those from C_P of Jacobs and Oonk (2001); this translates into a difference of about 10 J/(mol·K) at 2000 K. It is suggested that the newly obtained, larger C_P compared to those determined by the previous calorimetric measurements, greatly affects the value of Gibbs energy of Mg_2SiO_4 ringwoodite at high temperatures and high pressures. Re-investigation by a thermodynamic approach, particularly, on the phase boundary between Mg_2SiO_4 ringwoodite and $MgSiO_3$ perovskite + MgO will be needed as a future work.

ACKNOWLEDGMENTS

We thank Y.G. Yu and R.M. Wentzcovitch for providing the numerical data of calculated C_P for Mg_2SiO_4 ringwoodite and anonymous reviewers for useful comments. This study was supported in part by the Grants-in-Aid of the Scientific Research (No. 21540497 to H. Kojitani, No. 22340163 to M. Akaogi, and No. 20244086 to T. Inoue) of the Japan Society for the Promotion of Science.

REFERENCES CITED

Akaogi, M., Ross, N.L., McMillan, P., and Navrotsky, A. (1984) The Mg_2SiO_4 polymorphs (olivine, modified spinel and spinel)-thermodynamic properties from oxide melt solution calorimetry, phase relations, and models of lattice vibrations. American Mineralogist, 69, 499–512.

Akaogi, M., Takayama, H., Kojitani, H., Kawaji, H., and Atake, T. (2007) Low-temperature heat capacities, entropies and enthalpies of Mg_2SiO_4 polymorphs, and α-β-γ and post-spinel phase relations at high pressure. Physics and Chemistry of Minerals, 34, 169–183.

Akaogi, M., Kojitani, H., Morita, T., Kawaji, H., and Atake, T. (2008) Low-temperature heat capacities, entropies and high-pressure phase relations of $MgSiO_3$ ilmenite and perovskite. Physics and Chemistry of Minerals, 35, 287–297.

Anderson, O.L. and Isaak, D.G. (1995) Elastic constants of mantle minerals at high temperature, In T.J. Ahrens, Ed., Mineral Physics and Crystallography: A Handbook of Physical Constants, p. 64–97. AGU Reference shelf 2, American Geophysical Union, Washington, D.C.

Ashida, T., Kume, S., and Ito, E. (1987) Thermodynamic aspects of phase boundary among α-, β- and γ-Mg_2SiO_4. In M.H. Manghnani and Y. Syono, Eds., High-pressure Research in Mineral Physics, p. 269–274. Terra Scientific Publishing, Tokyo/American Geophysical Union, Washington D.C.

Ashida, T., Kume, S., Ito, E., and Navrotsky, A. (1988) $MgSiO_3$ ilmenite: Heat capacity, thermal expansivity, and enthalpy of transformation. Physics and Chemistry of Minerals, 16, 239–245.

Bina, C.R. and Wood, B.J. (1987) Olivine-spinel transitions: Experimental and thermodynamic constraints and implications for the nature of the 400-km seismic discontinuity. Journal of Geophysical Research, 92, 4853–4866.

Chopelas, A. (1999) Estimates of mantle relevant Clapeyron slopes in the $MgSiO_3$ system from high-pressure spectroscopic data. American Mineralogist, 84, 233–244.

Chopelas, A., Boehler, R., and Ko, T. (1994) Thermodynamics and behavior of γ-Mg_2SiO_4 at high pressure: Implications for Mg_2SiO_4 phase equilibrium. Physics and Chemistry of Minerals, 21, 351–359.

Ditmars, D.A., Ishihara, S., Chang, S.S., Bernstein, G., and West, E.D. (1982) Enthalpy and heat-capacity standard reference material: synthetic sapphire (α-Al_2O_3) from 10 to 2250 K. Journal of Research of the National Bureau of Standards, 87, 159–163.

Fabrichnaya, O.B., Saxena, S.K., Richet, P., and Westrum, E.F. (2004) Thermodynamic Data, Models and Phase Diagrams in Multicomponent Oxide Systems, 198 p. Springer, Berlin.

Fei, Y. and Saxena, S.K. (1986) A thermochemical data base for phase equilibria in the system Fe-Mg-Si-O at high pressure and temperature. Physics and Chemistry of Minerals, 13, 311–324.

——— (1987) An equation for the heat capacity of solid. Geochimica et Cosmochimica Acta, 51, 251–254.

Gillet, P., Richet, P., Guyot, F., and Fiquet, G. (1991) High-temperature thermodynamic properties of forsterite. Journal of Geophysical Research, 96, 11805–11816.

Higo, Y., Inoue, T., Li, B., Irifune, T., and Liebermann, R.C. (2006) The effect of iron on the elastic properties of ringwoodite at high pressure. Physics of the Earth and Planetary Interiors, 159, 276–285.

Hofmeister, A.M. and Ito, E. (1992) Thermodynamic properties of $MgSiO_3$ ilmenite from vibrational spectra. Physics and Chemistry of Minerals, 18, 423–432.

Inoue, T., Tanimoto, Y., Irifune, T., Suzuki, T., Fukui, H., and Ohtaka, O. (2004) Thermal expansion of wadsleyite, ringwoodite, hydrous wadsleyite and hydrous ringwoodite. Physics of the Earth and Planetary Interiors, 143–144, 279–290.

Jackson, J.M., Sinogeikin, S.V., and Bass, J.D. (2000) Sound velocities and elastic properties of γ-Mg_2SiO_4 to 873 K by Brillouin spectroscopy. American Mineralogist, 85, 296–303.

Jacobs, M.H.G. and Oonk, H.A.J. (2001) The Gibbs energy formulation of the α, β, and γ forms of Mg_2SiO_4 using Grover, Getting and Kennedy's empirical relation between volume and bulk modulus. Physics and Chemistry of Minerals, 28, 572–585.

Kajiyoshi, K. (1986) High-temperature equation of state for mantle minerals and their anharmonic properties. M.S. thesis, Okayama University, Japan.

Karki, B.B. and Wentzcovitch, R.M. (2002) First-principles lattice dynamics and thermoelasticity of $MgSiO_3$ ilmenite at high pressure. Journal of Geophysical Research, 107(B11), 2267, doi:10.1029/2001JB000702.

Katsura, T., Yoneda, A., Yamazaki, D., Yoshino, T., and Ito, E. (2010) Adiabatic temperature profile in the mantle. Physics of the Earth and Planetary Interiors, 183, 212–218.

Kieffer, S.W. (1979a) Thermodynamics and lattice vibrations of minerals: 1. Mineral heat capacities and their relationships to simple lattice vibrational models. Reviews of Geophysics and Space Physics, 17, 1–19.

——— (1979b) Thermodynamics and lattice vibrations of minerals: 3. Lattice dynamics and an approximation for minerals with application to simple substances and framework silicates. Reviews of Geophysics and Space Physics, 17, 35–59.

Li, B. (2003) Compressional and shear wave velocities of ringwoodite γ-Mg_2SiO_4 to 12 GPa. American Mineralogist, 88, 1312–1317.

McMillan, P. and Akaogi, M. (1987) Raman spectra of β-Mg_2SiO_4 (modified spinel) and γ-Mg_2SiO_4 (spinel). American Mineralogist, 72, 361–364.

Meng, Y., Fei, Y., Weidner, D.J., Gwanmesia, G.D., and Hu, J. (1994) Hydrostatic compression of γ-Mg_2SiO_4 to mantle pressures and 700 K: Thermal equation of state and related thermoelastic properties. Physics and Chemistry of Minerals, 21, 407–412.

Mraw, S.C. and Naas, D.F. (1979) The measurement of accurate heat capacities by differential scanning calorimetry. Comparison of d.s.c. results on pyrite (100 to 800 K) with literature values from precision adiabatic calorimetry. Journal of Chemical Thermodynamics, 11, 567–584.

Orr, R.L. (1953) High temperature heat contents of magnesium orthosilicate and ferrous orthosilicate. Journal of the American Chemical Society, 75, 528–529.

Ottonello, G., Civalleri, B., Ganguly, J., Vetuschi Zuccolini, M., and Noel, Y. (2009) Thermophysical properties of the α-β-γ polymorphs of Mg_2SiO_4: A computational study. Physics and Chemistry of Minerals, 36, 87–106.

Price, G.D., Parker, S.C., and Leslie, M. (1987) The lattice dynamics and thermodynamics of the Mg_2SiO_4 polymorphs. Physics and Chemistry of Minerals, 15, 181–190.

Robie, R.A., Hemingway, B.S., and Takei, H. (1982) Heat capacities and entropies of Mg_2SiO_4, Mn_2SiO_4, and Co_2SiO_4 between 5 and 380 K. American Mineralogist, 67, 470–482.

Sasaki, S., Prewitt, C.T., Sato, Y., and Ito, E. (1982) Single-crystal X-ray study of γ-Mg_2SiO_4. Journal of Geophysical Research, 87, 7829–7832.

Saxena, S.K., Chatterjee, N., Fei, Y., and Shen, G. (1993) Thermodynamic Data of Oxides and Silicates, 428 p. Springer, Berlin.

Suzuki, I., Ohtani, E., and Kumazawa, M. (1979) Thermal expansion of γ-Mg_2SiO_4. Journal of Physics of the Earth, 27, 53–61.

Watanabe, H. (1982) Thermochemical properties of synthetic high-pressure compounds relevant to the Earth's mantle. In S. Akimoto and M.H. Manghnani, Eds., High-pressure Research in Geophysics, p. 441–464. Center for Academic Publications, Tokyo, Japan.

Weidner, D.J., Sawamoto, H., Sasaki, S., and Kumazawa, M. (1984) Single-crystal elastic properties of the spinel phase of Mg_2SiO_4. Journal of Geophysical Research, 89, 7852–7860.

Yu, Y.G. and Wentzcovitch, R.M. (2006) Density functional study of vibrational and thermodynamic properties of ringwoodite, Journal of Geophysical Research, 111, B12202, doi:10.1029/2006JB004282.

MANUSCRIPT RECEIVED NOVEMBER 17, 2011
MANUSCRIPT ACCEPTED APRIL 9, 2012
MANUSCRIPT HANDLED BY SERGIO SPEZIALE